Long non-coding RNA FGD5-AS1/microRNA-133a-3p upregulates aquaporin 1 to decrease the inflammatory response in LPS-induced sepsis

YURU CHU[1*], XU WANG[2*], NAIHAO YU[1], YALI LI[1] and JIANYING KAN[1]

[1]Intensive Care Unit; [2]Acupuncture Department, Tianjin Academy of Traditional Chinese Medicine Affiliated Hospital, Tianjin 300120, P.R. China

Received December 17, 2020; Accepted April 19, 2021

DOI: 10.3892/mmr.2021.12424

Abstract. Sepsis is a systemic inflammatory response syndrome caused by infections. The present study aimed to investigate the potential mechanism of FGD5-AS1 in sepsis and lipopolysaccharide (LPS)-induced inflammatory response. An animal model of sepsis was constructed. LPS was used to induce mice HL-1 cardiomyocytes to construct a cell model. The association between FGD5-AS1 and miR-133a-3p was investigated through animal and cell models. FGD5-AS1 overexpression was used to analyze the effect of FGD5-AS1 on inflammatory reaction. Tumor necrosis factor (TNF)-α, interleukin (IL)-1β and IL-6 levels were detected by enzyme-linked immunosorbent assay and reverse transcription-quantitative polymerase chain reaction. The interaction of FGD5-AS1, miR-133a-3p and aquaporin 1 (AQP1) was detected by dual-luciferase reporter assay and microRNA (miRNA/miR) pull-down assay. Compared with the control group, the expression of FGD5-AS1 was decreased and the expression of miR-133a-3p was increased in the sepsis group. FGD5-AS1 overexpression increased LPS-induced expression of FGD5-AS1 and AQP1, decreased the expression of miR-133a-3p, and inhibited the expression of the inflammatory cytokines, TNF-α, IL-6 and IL-1β. Dual-luciferase reporter and miRNA pull-down assays confirmed the interaction of FGD5-AS1, miR-133a-3p and AQP1. These results indicated that FGD5-AS1 is the competitive endogenous RNA of miR-133a-3p on AQP1, and thus FGD5-AS1 overexpression may be able to inhibit the inflammatory response in sepsis.

Correspondence to: Dr Jianying Kan, Intensive Care Unit, Tianjin Academy of Traditional Chinese Medicine Affiliated Hospital, 354 Beima Road, Hongqiao, Tianjin 300120, P.R. China
E-mail: jykanyh@yeah.net

*Contributed equally

Key words: sepsis, FGD5-AS1, microRNA-133a-3p, aquaporin 1, competitive endogenous RNA

Introduction

Sepsis is a systemic inflammatory disease caused by severe trauma, burn, infection and major surgery (1-3). Sepsis is often accompanied by multiple organ failure (4). Sepsis-induced excessive inflammation, immunosuppression or excessive tissue damage may increase susceptibility to secondary infection (5). Therefore, the molecules and mechanisms associated with sepsis-induced inflammatory response are important to explore. Septic shock is associated with half of patients with septic myocarditis (6); inflammatory cytokines play an important role in this process. Among them, tumor necrosis factor (TNF-α) inhibits myocardial contractility, which results in cardiac dysfunction (7).

Long non-coding RNA (lncRNA) plays an important regulatory role in the occurrence and development of inflammatory response, rheumatoid arthritis, vascular aging and cancer (8,9). LncRNA IL-1β7R is involved in the inflammatory response induced by bacterial endotoxin lipopolysaccharide (LPS) (7). LncRNA HOTAIR promotes TNF-α production in mice with LPS-induced sepsis (4). FGD5-AS1 has low expression level in periodontitis, and FGD5-AS1 overexpression could inhibit the development of periodontitis (10). However, reports on the mechanism of action of FGD5-AS1 and its role in sepsis are few.

MicroRNAs (miRNAs/miRs) are single-stranded endogenous non-coding RNAs with a length of 18-25 nt (11). miRNAs are involved in gene expression, cell development, differentiation and other processes. miRNAs also play an important role in autoimmune diseases (12,13). Feng *et al* (14) found that miRNA plays an important role in the development of liver fibrosis. miR-133a-3p belongs to the myocyte-specific miR-206 family and inhibits the proliferation and differentiation of myocytes (15). In addition, miR-133a has been identified as a tumor suppressor gene in several tumors, such as colorectal cancer, ovarian cancer, breast cancer and bladder cancer (16-18). However, the role of miR-133a-3p in sepsis has been rarely reported. Aquaporin 1 (AQP1) belongs to a small-molecule transmembrane protein family, which is involved in the rapid transmembrane transport of water (19). AQP1 is one of the earliest identified members and expressed in erythrocyte membrane and vascular endothelial cells (20). AQP1 plays an important role in cell migration, differentiation,

proliferation and ion transport (21). AQP1 is a channel for the exchange of intracellular and extracellular water and the transport and exchange of oxygen in erythrocytes (22). The function of AQP1 is not only limited to the membrane aquaporin, and its abnormal expression is closely associated with the occurrence and development of a variety of common diseases (23-25).

In the present study, LPS was used to establish animal and cell models of sepsis, and the expression levels of FGD5-AS1, miR-133a-3p and AQP1 in cells were detected; their effect on sepsis and mechanism of action were also explored. The present study lays a theoretical foundation for further revealing the molecular mechanism of sepsis occurrence and development.

Materials and methods

Establishment of animal models of sepsis. A total of 36 female BALB/C mice (weight, 25-30 g; age, 4-6 weeks old) were purchased from Charles River Co., Ltd. Six mice were included in each group. The mice were raised in a sterile environment at a room temperature of 26-28˚C, a humidity of 50-60%, and illumination time of 10 h. The mice had free access to autoclaved water and sterile food. The experiment was conducted after 1 week of adaptive feeding. The control group was intraperitoneally injected with 5 ml/kg sterile saline. The model group was intraperitoneally injected with 15 mg/kg LPS (a bacterial endotoxin, *Escherichia coli* LPS serotype 0111:B4; Sigma-Aldrich; Merck KGaA). Len-NC and Len-FGD5-AS1 ($1x10^9$ PFU/ml), were injected into the tail vein after 24 h of modeling. The control group was given an equal volume of sterilized saline. All indexes were detected 24 h after caudal vein administration. A 0.3% pentobarbital sodium solution was given at a dose of 50 mg/kg to anesthetize the mice. Then, 0.2 ml of blood was collected from the orbital vein, and the upper serum was collected after centrifugation (4,000 x g, 10 min, 4˚C). The mice were euthanized with carbon dioxide immediately after blood extraction while still under anesthesia. The euthanasia chamber was filled with CO_2 at a rate of 20% of the volume of the euthanasia chamber per minute after the mice were placed in the chamber. The mice were not moving or breathing, and their pupils were dilated when the administration of CO_2 was stopped. The mice were watched for another 2 min to confirm their death. The animal experiments were approved by the Ethics Committee of Tianjin Academy of Traditional Chinese Medicine Affiliated Hospital (Tianjin, China; approval no. 20190135). The animal experiments were conducted between May 25 and June 14, 2019.

Lentiviral vector packaging. RNAi lentiviral recombinant vector system, including Len-FGD5-AS1 vector with green fluorescent protein (GFP), pHelper 1.0 vector and pHelper 2.0 vector and negative control lentivirus (Len-NC). All plasmid vectors were purchased from Shanghai GeneChem Co., Ltd. 293T cells in logarithmic growth phase were inoculated into the culture dish at a cell number of $6x10^6$/ml, and placed in an incubator for 24 h (CO_2, 37˚C). When the cell confluence reached 70-80%, each DNA solution (plasmid vector, helper plasmid vector pHelper 1.0, pHelper 2.0) and Lipofectamine® 2000 liposome were added for co-transfection. After 48 h, the supernatant of 293T cells was collected and centrifuged at 4,000 x g at 4˚C for 10 min. The supernatant was then filtered using a 0.45-μm diameter filter and packed. The 96-well plate was inoculated with $4x10^4$ cells per well. The virus was added into 8 experimental wells at a total volume of 100 μl by multiple dilution. Then, 24 h later, puromycin was added for screening, and the final concentration was 2.7 μg/ml. When the cell density reached 30%, lentivirus-transfected cells were transfected at a MOI of 30. A total of 16 h after lentivirus transfection, the solution was changed, and the downstream experiment was carried out after 96 h.

Cardiac function detection in mice. Cardiac function was evaluated using transthoracic Doppler ultrasound. Mice were prematurely fasted and weighed using a GE Vivid E9 ultrasound system (GE Healthcare). Mice were anesthetized to ideal depth and maintained with isoflurane (3% induction and 1-2% maintenance). The mice were fixed in supine position on a heating mat to maintain their body temperature, and the skin was prepared on the chest area. Measurement data: B-mode ultrasound was selected, and the left ventricle short axis image and the left ventricle long axis image were obtained at the left ventricle middle level using a high-frequency probe. Ejection fraction (EF%) and left ventricular fraction shorting rate (FS%) were measured under M-mode ultrasound. The data were measured three times, averaged and recorded.

Cell culture. Mice HL-1 cardiac muscle cells were purchased from the American Type Culture Collection. The cells were cultured in Dulbecco's modified Eagle's medium (Gibco; Thermo Fisher Scientific, Inc.) containing 10% fetal bovine serum (Gibco; Thermo Fisher scientific, Inc.) with 100 U/ml penicillin and 100 μg/ml streptomycin (Thermo Fisher Scientific, Inc.). The cells were precultured at 37˚C with 5% CO_2 for 24 h. LPS intervention was performed in some cells. These cells were plated in a 6-well plate ($2x10^6$) and cultured for 48 h, and then 1 g/ml LPS was added to the medium. Normal saline was added to the control group. The cells were cultured for 12 h under the same conditions. The harvested cells were used in subsequent experiments.

Cell transfection. The FGD5-AS1-pcDNA3.1-overexpression plasmid [vector-FGD5-AS1; OBiO Technology (Shanghai) Corp., Ltd.] was constructed in strict accordance with the manufacturer's instructions. A total of 4 μg vector-FGD5-AS1 and its negative control (vector-NC) were transfected into LPS-induced cells using Lipofectamine® 3000 (Thermo Fisher Scientific, Inc.) under 37˚C. The cells were collected after 48 h of transfection, and transfection efficiency was detected by reverse transcription-quantitative polymerase chain reaction (RT-qPCR). After 48 h of transfection, follow-up experiments were performed. Small interfering RNAs (siRNAs) targeting FGD5-AS1 (100 nM, 5'-CAUUUGUAAUAGUGUUCA AUA-3') and si-NC (100 nM, 5'-UUCUCCGAACGUGUCACG UTT-3') were synthesized by Shanghai GenePharma Co., Ltd., and transfected using Lipofectamine® 3000 (Thermo Fisher Scientific, Inc.). Vector-FGD5-AS1 (1 μg) and miR-133a-3p (100 nM) or sh-AQP1 (1 μg; Shanghai GenePharma Co., Ltd.) were co-transfected using Lipofectamine 3000. After 48 h of transfection, follow-up experiments were performed. Cells

were treated with 100 nM mimic control (5'-CAGCUGGUU GAAGGGGACCAAA-3') and 100 nM miR-133a-3p mimic (5'-UUUGGUCCCCUUCAACCAGCUG-3'). miRNAs were purchased from Shanghai GenePharma Co., Ltd.

Enzyme-linked immunosorbent assay (ELISA). Blood was drawn from the orbital venous plexus and centrifuged at 4˚C for 10 min (4,000 x g). The serum was separated and stored in the refrigerator at 80˚C for later use. The contents of TNF-α (cat. no. BMS607-3; Thermo Fisher Scientific, Inc.), interleukin (IL)-6 (cat. no. BMS603-2; Thermo Fisher Scientific, Inc.), and IL-1β (cat. no. BMS6002; Thermo Fisher Scientific, Inc.) in serum were detected by ELISA. ELISA was performed strictly in accordance with the manufacturer's instructions of the kits.

RT-qPCR. RNA from tissue or cell samples was isolated using TRIzol® reagent (Thermo Fisher Scientific, Inc.). RNA was reverse transcribed into cDNA using the PrimeScript One Step RT-PCR kit (Takara Biotechnology Co., Ltd.), according to the manufacturer's protocol. The reaction conditions for RT were as follows: 16˚C for 30 min, 42˚C for 30 min, 85˚C for 5 min. The following primers were used in the present study: miR-133a-3p forward, 5'-ACACTCCAGCTGGGTTGGTCCCCTTCAA CC-3' and reverse, 5'-CTCAACTGGTGTCGTGGAGTCGGC AATTCAGTTGAGACAGCTGG-3'; AQP1 forward, 5'-ACC TCCTGGCTATTGACTAC-3' and reverse, 5'-CCAGGATGA AGTCGTAGATG-3'; Bcl-2 forward, 5'-ATGCCTTTGTGG AACTATATGGC-3' and reverse, 5'-GGTATGCACCCAGAG TGATGC-3'; and Bax forward, 5'-TGAAGACAGGGGCCT TTTTG-3' and reverse, 5'-AATTCGCCGGAGACACTCG-3'. U6 RNA and GAPDH were used as the internal references. The primer sequences were as follows: U6 forward, 5'-CTCGCT TCGGCAgcacA-3' and reverse, 5'-aACGCttcacgaatttGCGT-3'; and GAPDH forward, 5'-GAGTCAACGGATTTGGTC GT-3' and reverse, 5'-TTgatttTGGATCTCG-3'. The fluorescence quantitative detection conditions were as follows: Pre-denaturation at 95˚C for 30 sec, amplification at 95˚C with extension for 15 sec, and 40 cycles of annealing at 60˚C for 30 sec. The $2^{-\Delta\Delta Cq}$ (26) was calculated as follows: ΔCq (experimental group)=Cq (experimental group target genes)-Cq (experimental group internal genes); ΔCq (control group)=Cq (control target gene)-Cq (control group).

Western blotting. HL-1 cells were collected after different treatments and lysed with RIPA lysis buffer (Beyotime Institute of Biotechnology), 100 μM PMSF (X100; Sigma-Aldrich; Merck KGaA) and a protease inhibitor cocktail (Thermo Fisher Scientific, Inc.). The lysed solution was centrifuged (12,000 x g) at 4˚C for 60 min and then at 12,000 x g for 20 min. PBS washing and precipitation were performed twice. Protein concentration was determined with the Bradford method. Then, 10 μg protein was added into 10% sodium dodecyl sulfate-polyacrylamide gel and subjected to electrophoresis. Subsequently, the gel was transferred to a polyvinylidene difluoride membrane, the membrane was then blocked with 5% skimmed milk powder at room temperature for 2 h. Following which, the membranes were incubated at 4˚C overnight with primary antibodies against the following: Bax (1:1,000; cat. no. 89477; Cell Signaling Technology, Inc.), Bcl-2 (1:1,000; cat. no. 15071; Cell Signaling Technology, Inc.), GAPDH (1:2,000; cat. no. 97166; Cell Signaling Technology, Inc.) and AQP1 (1:1,000; cat. no. ab9566; Abcam). Then, horseradish peroxidase-conjugated secondary antibodies (1:10,000; cat. nos. 31430 and 31460; Thermo Fisher Scientific, Inc.) were added to the membrane and incubated at room temperature for 2 h. Chemiluminescence (ECL kit; Cytiva) was used to detect the target bands. After the strips were scanned, the optical density of the strips was determined using QuantityOne version 4.3.0 software (Bio-Rad Laboratories, Inc.). The relative expression level of each sample was calculated using GADPH as the internal reference.

Cell counting Kit-8 (CCK-8) experiments. Cell viability was detected by the CCK-8 method. The cells were made into a single cell suspension and inoculated at a density of $1x10^5$/well to a 6-well plate. The cells were randomly grouped when cell confluence reached 60-70%. The control group was added with the corresponding volume of solvent. The LPS group was treated with 10 μg/ml LPS for 12 h. Lipofectamine® 2000 was used to transfect the target gene plasmid in the transfection group. The cells were incubated at 37˚C with 5% CO_2 for 48 h. CCK-8 experiment was performed after 48 h of cell treatment. CCK-8 reagent (Beyotime Institute of Biotechnology) was added to each well, and culture was continued for 4 h. The optical density at 490 nm was measured with a microplate reader.

Dual-luciferase reporter gene assay. StarBase version 2.0 (http://starbase.sysu.edu.cn/) online prediction software was used to predict the lncRNA-targeted miRNAs. TargetScan version 7.1 (http://www.targetscan.org/) online prediction software was used to predict the miRNA target genes. The interaction of the FGD5-AS1, miR-133a-3p and AQP1 cascade reaction was detected using a Dual-Luciferase Reporter Assay System (Promega Corporation). Wild-type (WT) and mutant (MT) 3'UTR were designed and amplified using Primer Premier 5.0 primer design software (Premier Biosoft International). *Xho*I and *Not*I were introduced into the 5' end of the WT forward primer and reverse primer, respectively. The WT and MT recombinant plasmids were constructed by ligating the vector psiCHECK™-2 with *Xho*I and *Not*I. Human 293T cells (American Type Culture Collection) were transfected with 100 nmol/μl miR-133a-3p mimics (5'-UUU GGUCCCCUUCAACCAGCUG-3') and its negative control (miR-NC; 5'-UUGUACUACACAAAAGUACUG-3'), 20 ng WT FGD5-AS1 (FGD5-AS1-WT) and MT FGD5-AS1 (FGD5-AS1-MT), or 20 ng 3'-untranslated region (UTR) of WT AQP1 (AQP1-WT) and MT AQP1 (AQP1-MT) with Lipofectamine® 3000 (Invitrogen; Thermo Fisher Scientific, Inc.). Luciferase activity was detected 48 h after transfection (Promega Corporation). According to the requirements of the kit instructions, the ratio of Firefly/*Renilla* luciferase activity was calculated. The unit of the control group ratio was one. The relative luciferase activity of different treatment groups was obtained.

miRNA pull-down experiment. miR-133a-3p mimic (biotinylated miR-133a-3p or miR-NC probe) with biotinylated modification was synthesized at the 3' ends. A random sequence was used as a control. Transfection with miR-133a-3p probe

(1 μg; Sangon Biotech Co., Ltd.) was performed, and cells were harvested after 48 h. The cells were washed with PBS and added with lytic extract (20 mM Tris, pH 7.5; 100 mM KCl; 5 mM $MgCl_2$; 0.5% NP-40; and 1 U/μl recombinant RNAse inhibitor). Cell fragments were removed by centrifugation after lysis (4˚C, 12,000 x g, 10 min). DNase l was added to the lysate to digest the DNA. Afterward, the lysates were heated to 65˚C in a metal bath for 5 min and then quickly plunged into ice to cool. The lysates and 25 μl avidin-coated magnetic beads (New England BioLabs, Inc.) were mixed and incubated at 4˚C for 4 h with gentle shaking. After incubation, the beads were washed twice with the lysis buffer. TRIzol was used to extract the RNA bound to the magnetic beads for RT-qPCR analysis. Cell lysate was used as a control (input group).

Statistical analysis. All data are expressed as the mean ± standard deviation. Comparison between two groups was performed using an unpaired Student's t-test. Differences between two groups were calculated using one-way analysis of variance (ANOVA) followed by Tukey's multiple comparison test. All data were statistically analyzed using SPSS 19.0 (SPSS, Inc.). Results were obtained from three independent experiments. P<0.05 was used to indicate a statistically significant difference.

Results

FGD5-AS1 is downregulated in sepsis. A septic animal model was established to investigate the role of FGD-AS1 in sepsis. Experimental results showed that FGD5-AS1 was downregulated in the septic animal model (Fig. 1A). Furthermore, a septic cardiomyocyte model was established using LPS. It was found that FGD5-AS1 was downregulated in the septic cell model (mouse HL-1 cells, Fig. 1B).

Lentivirus overexpression of FGD5-AS1 can inhibit sepsis. It was investigated whether FGD5-AS1 overexpression has a protective effect on sepsis. FGD5-AS1 was overexpressed in an animal model of sepsis by the lentivirus technique. The experimental results showed that the lentivirus overexpression system could upregulate the expression of FGD5-AS1 (Fig. 2A). Inflammatory factor detection results showed that the concentrations of TNF-α, IL-1β and IL-6 in the sepsis model group were significantly higher compared with those in the control group (P<0.01). The concentrations of TNF-α, IL-1β and IL-6 in the sepsis model + Len-FGD5-AS1 group was significantly decreased compared with the sepsis model + Len-NC group (P<0.01; Fig. 2B-D). Furthermore, it was found that FGD5-AS1 overexpression protected heart functions in septic mice. The ejection fraction, fractional shortening and the maximum [LVdP/dt (max)] and minimum rates of the rise in left ventricular pressure [LVdP/dt (min)] were significantly decreased in the sepsis model group compared with the control group (P<0.01; Fig. 2E-H). Ejection fraction, fractional shortening, LVdP/dt (max), and LVdP/dt (min) were significantly higher in the sepsis model + Len-FGD5-AS1 group compared with the sepsis model + Len-NC group (P<0.01; Fig. 2E-H).

FGD5-AS1 overexpression decreases LPS-induced HL-1 cell injury in vitro. A cell model was established by LPS, and the transfection efficiency of vector-FGD5-AS1 was first

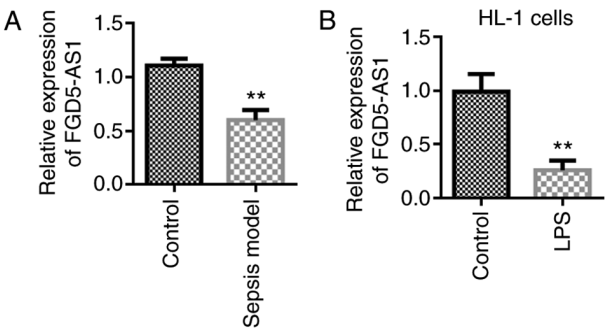

Figure 1. FGD5-AS1 is downregulated in sepsis. (A) FGD5-AS1 was downregulated in animal models of sepsis (arterial tissue of septic mice) (n=6). (B) FGD5-AS1 was downregulated in the sepsis cell model (mouse cardiomyocyte UL-1 cells). Results were obtained from three independent experiments, each performed in triplicate, the error bars represent SD. **P<0.01. LPS, lipopolysaccharide.

detected. Experimental results showed that vector-FGD5-AS1 could upregulate the expression of FGD5-AS1 (Fig. 3A). Subsequently, the effect of vector-FGD5-AS1 on cell viability was examined. The experimental results showed that transfection with vector-FGD5-AS1 could upregulate the viability of HL-1 cells compared with the vector-NC group (Fig. 3B). In addition, vector-FGD5-AS1 could inhibit Bax expression and upregulate Bcl-2 expression (Fig. 3C and D). The influence of FGD5-AS1 on the protein expression levels of Bax and Bcl-2 was further analyzed. The western blot analysis results were consistent with the RT-qPCR results; that is, vector-FGD5-AS1 transfection could inhibit Bax expression and upregulate Bcl-2 expression (Fig. 3C and D). Previous studies have shown that LPS treatment increases the levels of pro-inflammatory cytokines TNF-α, IL-6 and IL-1β (27-29). Transfection with vector-FGD5-AS1 in the cell models reverted LPS-induced changes in TNF-α, IL-6 and IL-1β levels (Fig. 3E-G).

Regulation and interaction of FGD5-AS1 on miR-133a-3p. lncRNA-targeted miRNA prediction analysis using StarBase showed that FGD5-AS1 has binding sites with miR-133a-3p (Fig. 4A). Dual-luciferase reporter gene validation results showed that miR-133a-3p significantly inhibited the luciferase activity of FGD5-AS1-WT (P<0.01). However, miR-133A-3p had no effect on the luciferase activity of FGD5-AS1-MT (Fig. 4B). miRNA pull-down also verified the interaction between FGD5-AS1 and miR-133a-3p (Fig. 4C). Subsequently, the effect of FGD5-AS1 on the expression of miR-133a-3p was detected. Following transfection with si-FGD5-AS1, FGD5-AS1 expression was found to be downregulated compared with the si-NC group, whereas transfection with vector-FGD5-AS1 increased the expression levels of FGD5-AS1 compared with the vector-NC group (Fig. 4D). Furthermore, the experimental results showed that transfection with vector-FGD5-AS1 inhibited miR-133a-3p expression, whereas si-FGD5-AS1 transfection led to the upregulation of miR-133a-3p (Fig. 4E). miR-133a-3p was also upregulated in septic animal models compared with the control group (Fig. 4F).

miR-133a-3p overexpression reverses the protective effect of FGD5-AS1 on HL-1 cells. After confirming the regulatory effect of FGD5-AS1 on miR-133a-3p, the effect of

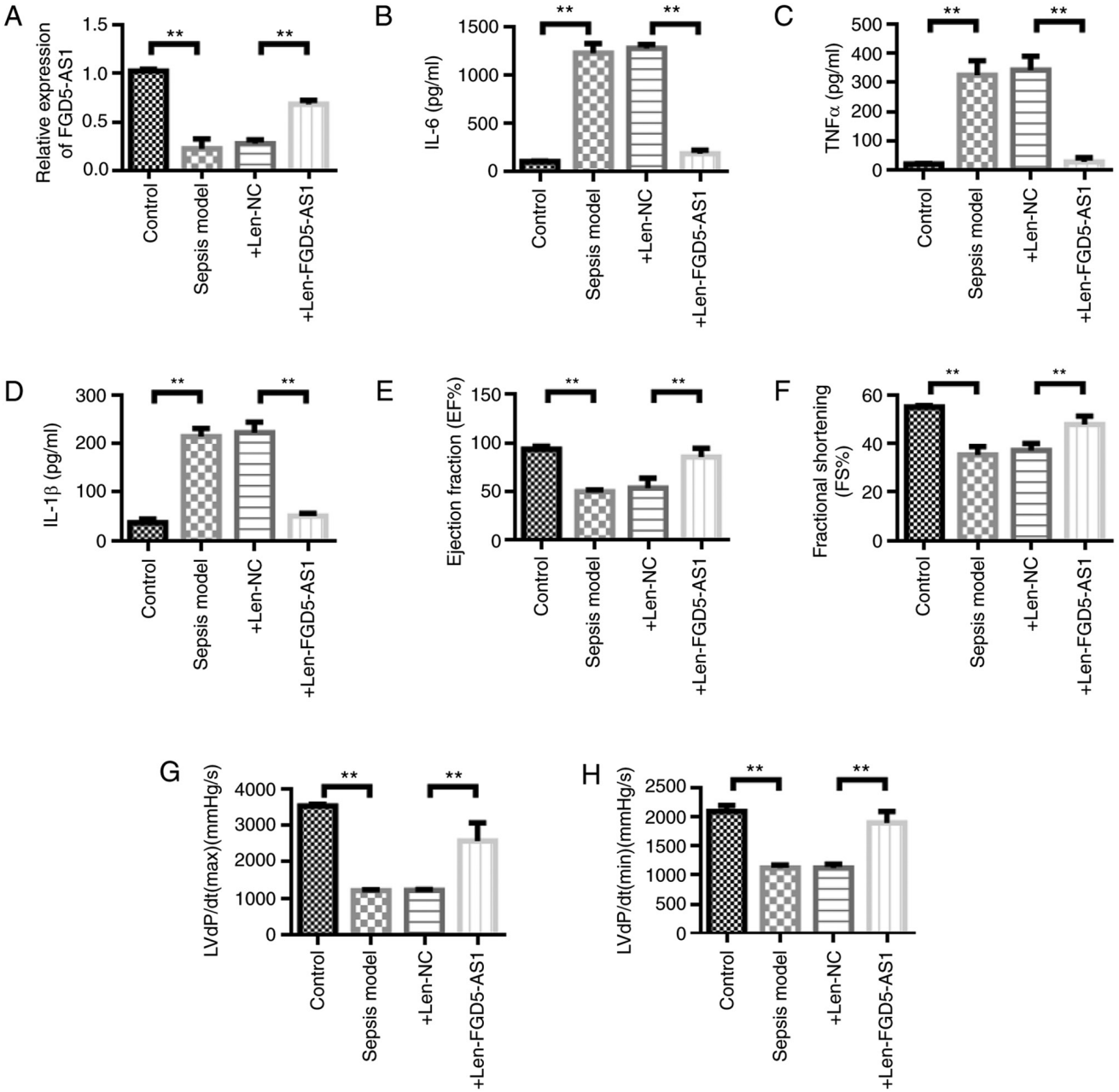

Figure 2. Lentiviral overexpression of FGD5-AS1 can inhibit sepsis. (A) Lentiviral overexpression of FGD5-AS1 could inhibit FGD5-AS1 expression in sepsis model mice. Detection of (B) IL-6, (C) TNF-α and (D) IL-1β activity in serum. (E) Detection of changes in mouse heart index (EF%). (F) Detection of changes in FS% of mouse heart index. (G) Detection of changes in mouse heart index LVdP/dt(max)(mmHg/sec). (H) Detection of changes in mouse heart indicators LVdP/dt(min)(mmHg/sec). n=6. Data are represented as the means ± SD. **P<0.01. Len-, lentivirus; IL, interleukin; TNF, tumor necrosis factor; EF, ejection fraction; FS, fractional shortening; NC, negative control; max, maximum; min, minimum; LVdP, left ventricular pressure.

miR-133a-3p on the function of FGD5-AS1 was detected. The viability of HL-1 cells was measured by CCK-8 assay. The results showed that the viability of HL-1 cells was decreased in the LPS-stimulated group compared with the control group. Transfection with vector-FGD5-AS1 could upregulate the viability of HL-1 cells compared with the LPS group. However, the viability of HL-1 cells was decreased after the co-transfection of vector-FGD5-AS1 and miR-133a-3p mimics (Fig. 5A). The Bax expression detection results showed that, compared with the LPS group, transfection with vector-FGD5-AS1 could inhibit Bax expression. However, Bax expression was upregulated after the co-transfection of vector-FGD5-AS1 and miR-133a-3p mimics (Fig. 5B). The trend in Bcl-2 expression changes was opposite to that of Bax. FGD5-AS1-vector transfection upregulated the expression of Bcl-2 (Fig. 5C). LPS stimulation upregulated the expression of inflammatory cytokines IL-6, TNF and IL-1β compared with the control group. Transfection with vector-FGD5-AS1 decreased the levels of inflammatory factors compared with the LPS group. However, the inflammatory factors were upregulated after the co-transfection of vector-FGD5-AS1 and miR-133a-3p mimics (Fig. 5D-F).

AQP1 acts as the target gene mediating miR-133a-3p expression. The complementary binding sites of miR-133a-3p and AQP1-3'-UTR-WT were predicted by TargetScan (Fig. 6A).

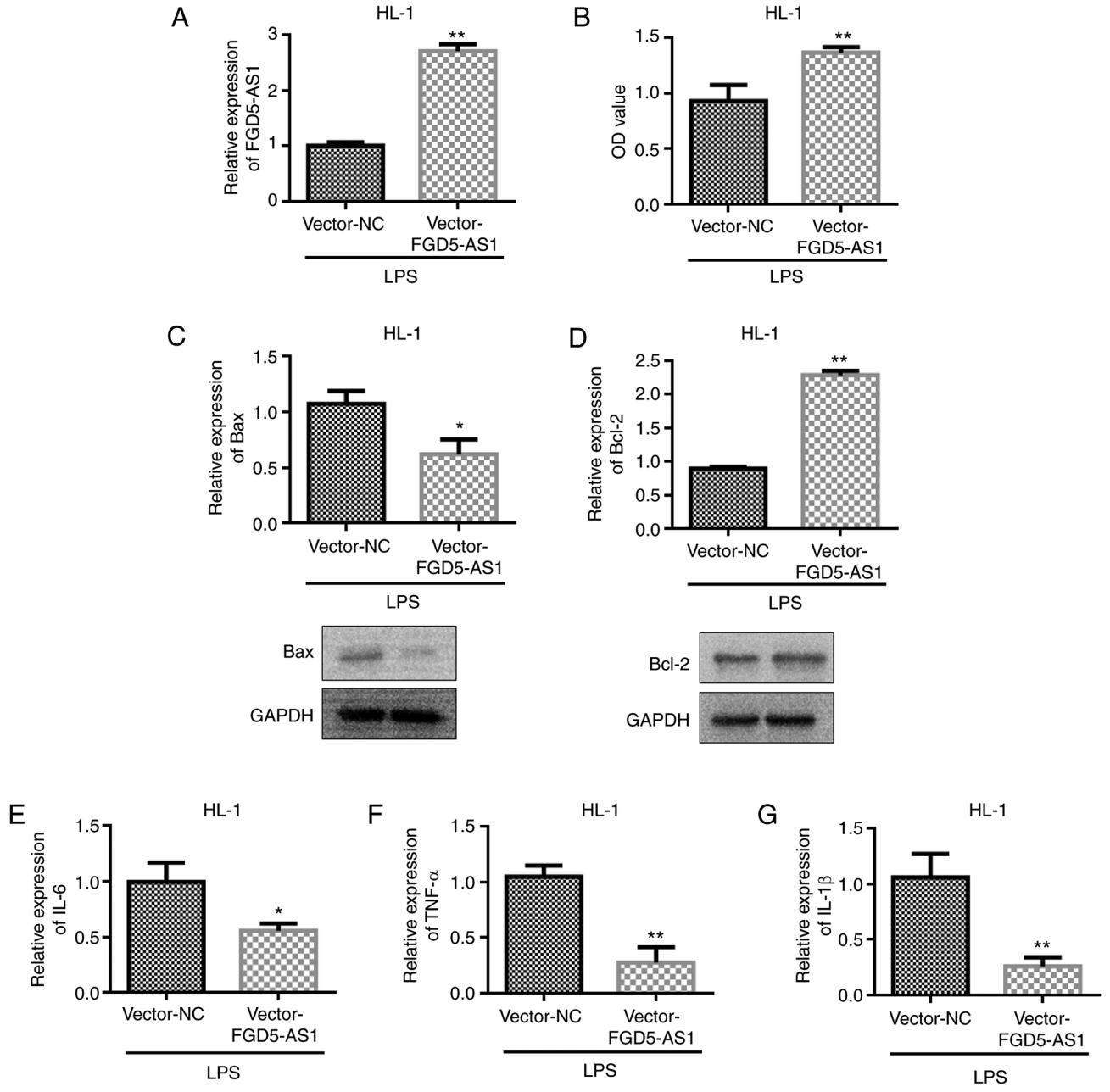

Figure 3. Overexpression of FGD5-AS1 decreases LPS-induced HL-1 cell damage. (A) Vector-FGD5-AS1 transfection efficiency test under LPS treatment conditions. (B) Cell Counting Kit-8 was performed to detect cell viability. Reverse transcription-quantitative PCR and western blotting was conducted to detect changes in (C) Bax expression and (D) Bcl-2 expression in cells after different treatments. Detection of (E) IL-6 expression, (F) TNF-α expression and (G) IL-1β activity in cells. Results were obtained from three independent experiments, each performed in triplicate, the error bars represent SD. *P<0.05, **P<0.01. NC, negative control; LPS, lipopolysaccharide; IL, interleukin; TNF, tumor necrosis factor.

Dual-luciferase reporter gene detection results showed that the relative luciferase activity of AQP1-WT + miR-133a-3p mimics group was significantly decreased compared with the AQP1-WT + miR-NC group (Fig. 6B). These results indicated that miR-133a-3p could inhibit luciferase activity by binding to AQP13'-UTR. However, the relative luciferase activity of the AQP1-MT + miR-133a-3p mimics group was not significantly different from that of the AQP1-MT + miR-NC group. These results indicated that miR-133a-3p and miR-NC could not inhibit the luciferase activity of the mutant plasmid. miRNA pull-down also verified the binding of miR-133a-3p to AQP1 (Fig. 6C). Subsequently, the effect of miR-133a-3p on the expression level of AQP1 was detected. Transfection with the miR-133a-3p mimics upregulated the expression of miR-133a-3p compared with the mimics-NC group, whereas transfection with the miR-133a-3p inhibitor led to the downregulation of miR-133a-3p expression compared with the inhibitor-NC (Fig. 6D). The experimental results showed that transfection with the miR-133a-3p mimics inhibited AQP1 expression, whereas AQP1 expression was upregulated in the miR-133a-3p inhibitor group (Fig. 6E). Transfection with vector-FGD5-AS1 upregulated AQP1 expression compared with the vector-NC group, whereas transfection with si-FGD5-AS1 led to the downregulation of AQP1 expression compared with the si-NC group (Fig. 6F). The western blotting results were consistent with the RT-qPCR

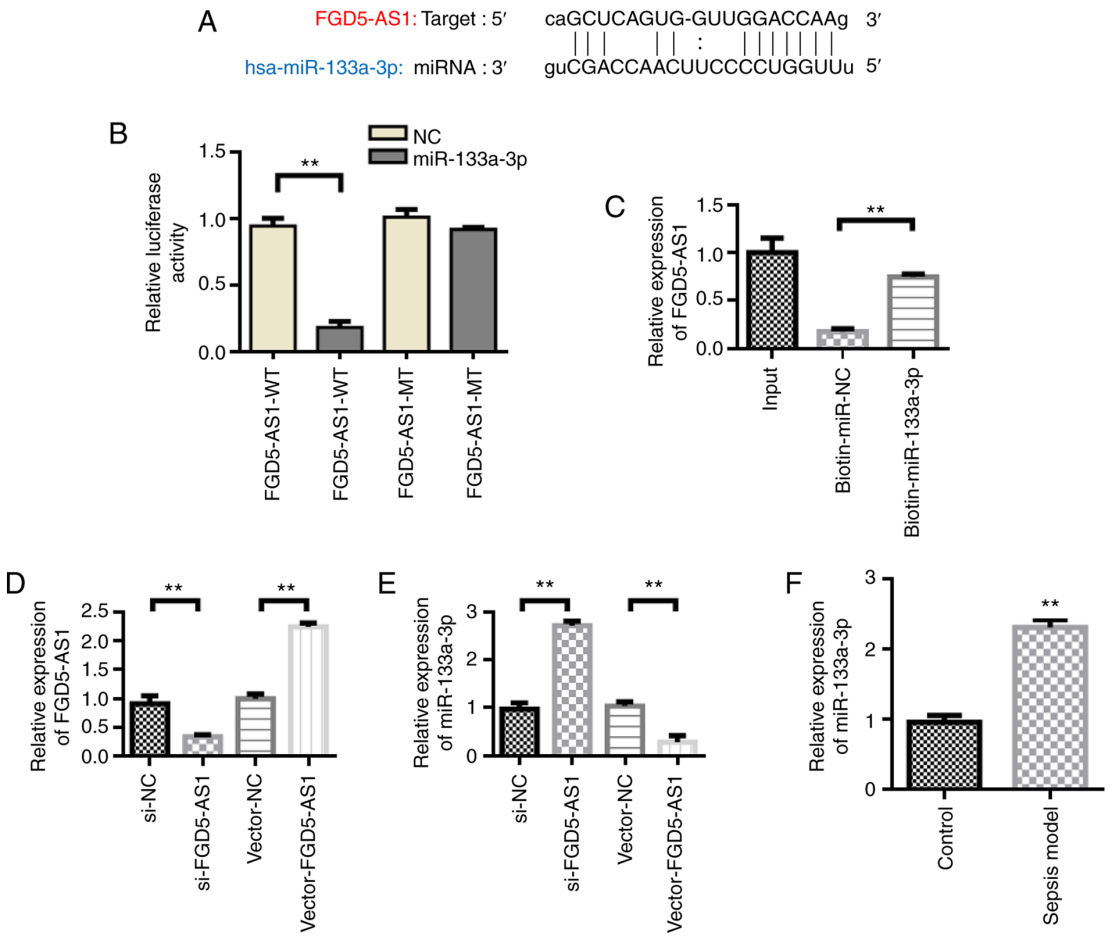

Figure 4. FGD5-AS1 acts as the competitive endogenous RNA of miR-133a-3p. (A) Schematic diagram of the binding site of FGD5-AS1 and miR-133a-3p. (B) The dual-luciferase reporter gene detection experiment verified the binding of FGD5-AS1 and miR-133a-3p. (C) miRNA pull-down assay verified the binding of FGD5-AS1 and miR-133a-3p. (D) Verification of transfection efficiency of overexpression and knockdown of FGD5-AS1. (E) Effects of FGD5-AS1 knockdown and overexpression on miR-133a-3p expression. (F) miR-133a-3p expression was upregulated in animal models of sepsis. Results were obtained from three independent experiments, each performed in triplicate, the error bars represent SD. **P<0.01. miRNA/miR, microRNA; WT, wild-type; MT, mutant; NC, negative control; si-, small interfering RNA.

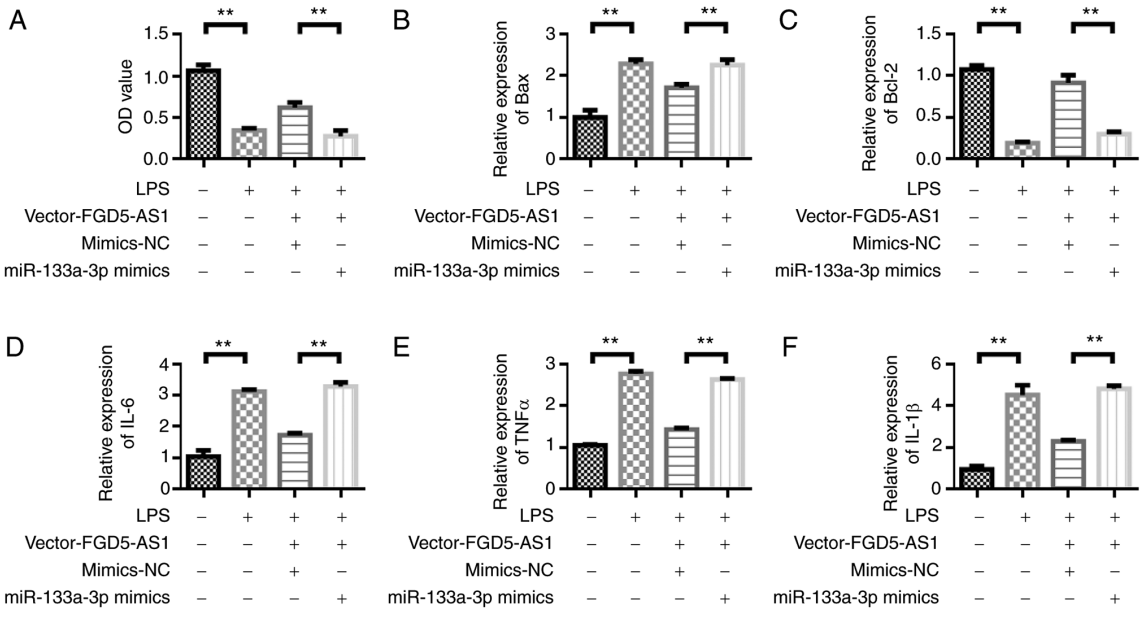

Figure 5. Overexpression of miR-133a-3p reverses the protective effect of FGD5-AS1 on HL-1 cells. (A) Cell Counting Kit-8 detection of cell viability. Reverse transcription-quantitative PCR was performed to detect the expression of (B) Bax, (C) Bcl-2, (D) IL-6, (E) TNF-α and (F) IL-1β. Results were obtained from three independent experiments, each performed in triplicate, the error bars represent SD. **P<0.01. miR, microRNA; IL, interleukin; TNF, tumor necrosis factor; NC, negative control; LPS, lipopolysaccharide.

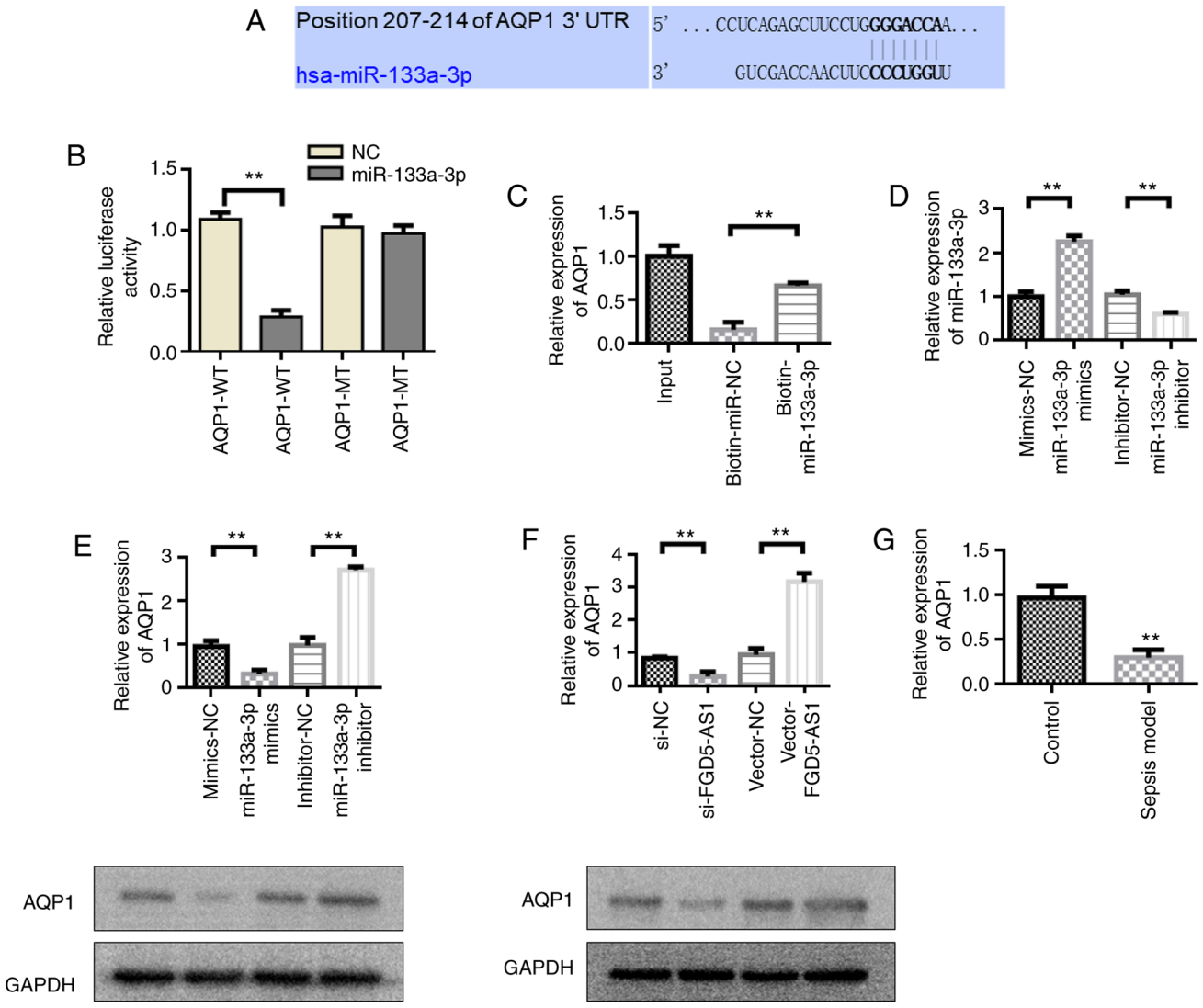

Figure 6. AQP1 as a target gene that mediates miR-133a-3p. (A) Schematic diagram of the binding between miR-133a-3p and AQP1. (B) The dual-luciferase reporter assay was performed to detect the binding of miR-133a-3p to AQP1. (C) miRNA pull-down assay verified the binding of miR-133a-3p to AQP1. (D) Verification of transfection efficiency of miR-133a-3p mimics and inhibitors. (E) Effects of miR-133a-3p knockdown and overexpression on the expression of AQP1. (F) Effects of FGD5-AS1 overexpression and knockdown on the expression of AQP1. (G) AQP1 was downregulated in the sepsis model. Results were obtained from three independent experiments, each performed in triplicate, the error bars represent SD. **P<0.01. AQP1, aquaporin 1; UTR, untranslated region; miR/miRNA, microRNA; WT, wild-type; MT, mutant; NC, negative control; si-, small interfering RNA.

results (Fig. 6F). AQP1 was downregulated in septic animal models (Fig. 6G).

AQP1 knockdown reverses the protective effect of FGD5-AS1 on HL-1 cells. RT-qPCR was used to detect the change in AQP1 expression (Fig. S1). FGD5-AS1-vector transfection could upregulate AQP1 expression, but the expression of AQP1 was decreased after the addition of sh-AQP1 (Fig. 7A). The viability of HL-1 cells was measured by CCK-8 assay. The results showed that the viability of HL-1 cells was decreased in the LPS-stimulated group compared with the control group. Transfection with vector-FGD5-AS1 could upregulate the viability of HL-1 cells compared with the LPS group. However, the viability of HL-1 cells decreased after the co-transfection of vector-FGD5-AS1 + sh-AQP1 (Fig. 7B). The Bax expression detection results showed that, compared with the LPS group, vector-FGD5-AS1 transfection could inhibit Bax expression. However, Bax expression was upregulated after the co-transfection of vector-FGD5-AS1 + sh-AQP1 (Fig. 7C). The change in Bcl-2 expression was opposite to that of Bax. Vector-FGD5-AS1 transfection upregulated Bcl-2 expression (Fig. 7D). LPS stimulation upregulated the expression of inflammatory cytokines IL-6, TNF and IL-1β compared with the control group. Transfection with vector-FGD5-AS1 decreased the levels of inflammatory factors compared with the LPS group. However, the inflammatory factors were upregulated after the co-transfection of vector-FGD5-AS1 + sh-AQP1 (Fig. 7E-G). Fig. 7H illustrates the proposed underlying mechanism for the signaling pathway that involves FGD-AS1-miR-133a-3p-AQP1 in sepsis.

Discussion

Sepsis is a systemic inflammatory response caused by infection that leads to multiple organ failure, in which the heart

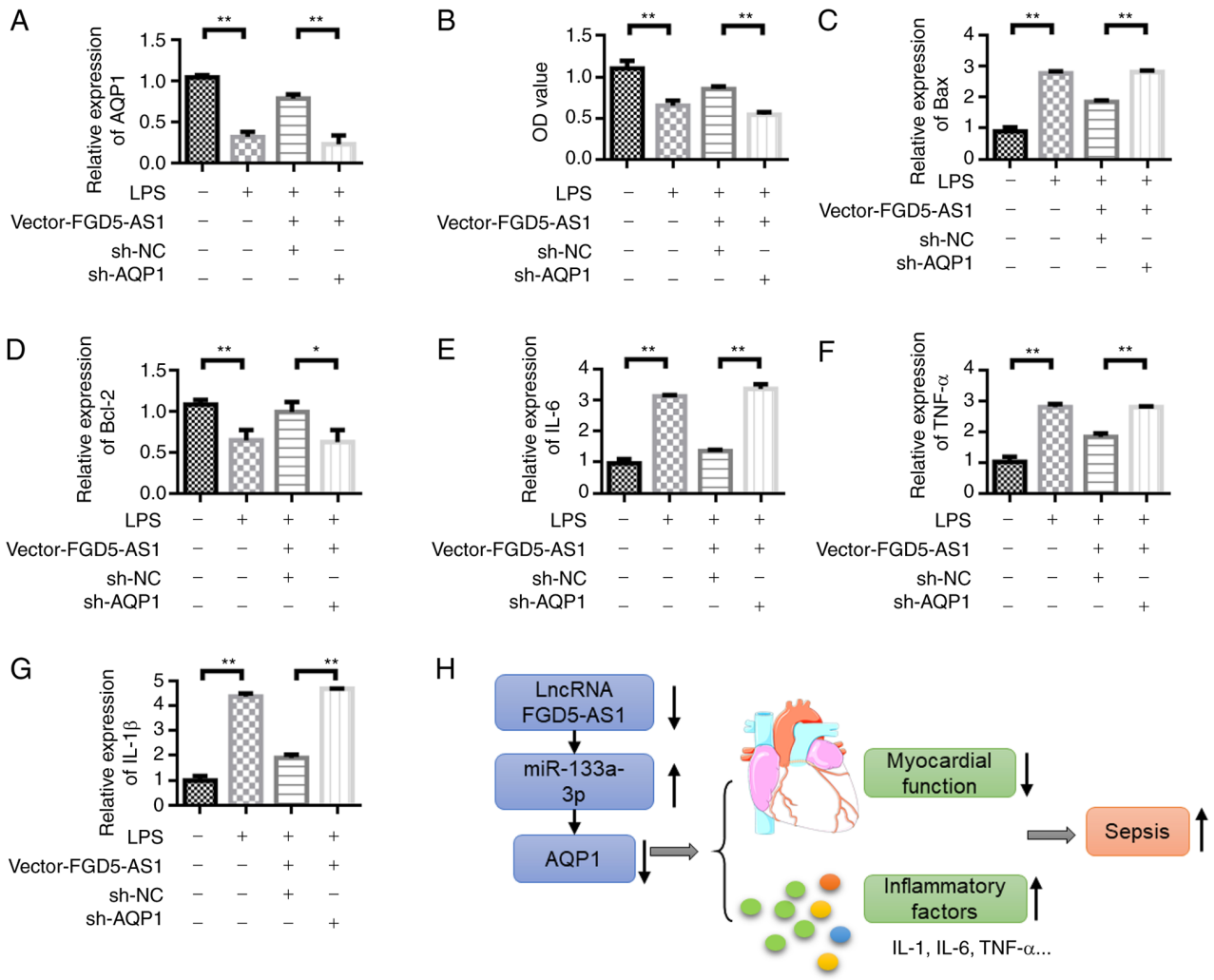

Figure 7. Knockdown of AQP1 reverses the protective effect of FGD5-AS1 on HL-1 cells. (A) Detection of AQP1 expression level in HL-1 cells under different treatment conditions. (B) Cell Counting Kit-8 cell viability detection. Reverse transcription-quantitative PCR was performed to detect the expression of (C) Bax, (D) Bcl-2, (E) IL-6, (F) TNF-α and (G) IL-1β. (H) Schematic diagram of the proposed mechanisms of the signaling pathway involving FGD-AS1-miR-133a-3p-AQP1 in sepsis. Results were obtained from three independent experiments, each performed in triplicate, the error bars represent SD. *P<0.05, **P<0.01. AQP1, aquaporin 1; IL, interleukin; TNF, tumor necrosis factor; miR, microRNA; NC, negative control; sh-, short hairpin RNA; LPS, lipopolysaccharide; lncRNA, long non-coding RNA.

is one of the most vulnerable organs (30,31). Current treatments, such as antimicrobial therapy and supportive therapies, are still at the early stages (32,33). The study of non-coding RNA provides a novel idea for the treatment of myocardial inflammation caused by sepsis (4,34).

The role of non-coding RNA in physiological and pathological processes, including cell proliferation, apoptosis, inflammatory response and immunity, has received extensive attention (35). Studies have shown that lncRNAs play a crucial role in a number of inflammatory diseases, such as sepsis (36,37). For example, lncRNA growth arrest specific transcript 5 is involved in regulating sepsis-induced podocyte injury by inhibiting the expression of phosphatase and tension protein homologous gene (38). In addition, miRNAs are valuable markers for the diagnosis and prognosis of sepsis. Lan *et al* (39) showed that the expression of serum miR-155-5p and miR-133a-3p could be used as a specific indicator for the diagnosis of sepsis. Further results showed that the expression of miR-155-5p could be an independent influencing factor for the prognosis of sepsis (39).

In the present study, *in vitro* cell models were used to investigate the expression and mechanism of FGD5-AS1 in sepsis inflammatory response. Experiments confirmed that plasma FGD5-AS1 expression decreased, miR-133a-3p expression increased, AQP1 expression was downregulated, and the release of serum proinflammatory cytokines was increased in the sepsis model. Inflammatory cytokines are involved in sepsis-induced myocardial damage. Studies have shown that TNF-α and IL-1β initiate an inflammatory response that has a negative inotropic effect on the myocardium (40,41). The negative regulation of IL-6 on myocardial systolic performance is associated through the protein kinase pathway (42,43). In the present study, FGD5-AS1 overexpression inhibited the expression of inflammatory cytokines TNF-α, IL-1β and IL-6 in the sepsis models. Thus, these results indicated that FGD5-AS1 is involved in the regulation of the expression of inflammatory cytokines.

In the present study, miR-133a-3p was upregulated in the blood samples of LPS mice. These results suggested that miR-133a-3p plays a regulatory role in sepsis-induced

inflammatory response. Further results confirmed that miR-133a-3p and its predicted target gene AQP1 were remarkably upregulated in plasma and downregulated in the LPS-induced cells, respectively. AQP1 plays an important regulatory role in the inflammatory response caused by neonatal toxic erythema, rheumatoid arthritis and pulmonary edema (44-46). Thus, AQP1 can regulate inflammatory response. In the present study, FGD5-AS1 overexpression decreased LPS-induced upregulation of TNF-α, IL-6 and IL-1β by upregulating AQP1. This result suggested that FGD5-AS1 and miR-133a-3p are antagonistic regulators of AQP1 expression and inflammatory response. FGD5-AS1 was indicated to have a protective effect on sepsis-induced inflammatory response.

In summary, the present study focused on the mechanisms and signaling pathways that regulate inflammatory responses in sepsis and investigated whether FGD5-AS1 is a potential therapeutic target for sepsis and complications. In the present study, FGD5-AS1 and AQP1 expression was decreased in animal models of sepsis, and LPS-induced cells; the expression of miR-133a-3p was increased. Pro-inflammatory cytokines TNF-α, IL-6 and IL-1β were remarkably elevated in LPS-induced cells. FGD5-AS1 overexpression could reverse LPS-induced changes in the levels of miR-133a-3p, AQP1 and pro-inflammatory factors. Therefore, these results indicated that FGD5-AS1 is the competing endogenous RNA of miR-133a-3p on AQP1.

Acknowledgements

Not applicable.

Funding

No funding was received.

Availability of data and materials

The datasets used and/or analyzed in the current study are available from the corresponding author on reasonable request.

Authors' contributions

JK designed the experiments. YC and XW performed the experiments and data analysis. YC, NY and YL performed data analysis and wrote the manuscript, with contributions from all authors. YC and JK confirm the authenticity of all the raw data. All authors read and approved the final manuscript.

Ethics approval and consent to participate

The animal experiments were approved by the Ethics Committee of Tianjin Academy of Traditional Chinese Medicine Affiliated Hospital (Tianjin, China; grant no. 20190135).

Patient consent for publication

Not applicable.

Competing interests

The authors declare that they have no competing interests.

References

1. Russell JA: Management of sepsis. N Engl J Med 355: 1699-1713, 2006.
2. Bone RC: The pathogenesis of sepsis. Ann Intern Med 115: 457-469, 1991.
3. IDSA Sepsis Task Force: Infectious diseases society of America (IDSA) position statement: Why IDSA did not endorse the surviving sepsis campaign guidelines. Clin Infect Dis 66: 1631-1635, 2018.
4. Wu H, Liu J, Li W, Liu G and Li Z: LncRNA-HOTAIR promotes TNF-α production in cardiomyocytes of LPS-induced sepsis mice by activating NF-κB pathway. Biochem Biophys Res Commun 471: 240-246, 2016.
5. Cawcutt KA and Peters SG: Severe sepsis and septic shock: Clinical overview and update on management. In: Mayo Clinic Proceedings, Elsevier, pp1572-1578, 2014.
6. Rudiger A and Singer M: Mechanisms of sepsis-induced cardiac dysfunction. Crit Care Med 35: 1599-1608, 2007.
7. Guo W, Liu W, Chen G, Hong S, Qian C, Xie N, Yang X, Sun Y and Xu Q: Water-soluble andrographolide sulfonate exerts anti-sepsis action in mice through down-regulating p38 MAPK, STAT3 and NF-κB pathways. Int Immunopharmacol 14: 613-619, 2012.
8. Yang F, Xue X, Bi J, Zheng L, Zhi K, Gu Y and Fang G: Long noncoding RNA CCAT1, which could be activated by c-Myc, promotes the progression of gastric carcinoma. J Cancer Res Clin Oncol 139: 437-445, 2013.
9. Pearson MJ and Jones SW: Review: Long noncoding RNAs in the regulation of inflammatory pathways in rheumatoid arthritis and osteoarthritis. Arthritis Rheumatol 68: 2575-2583, 2016.
10. Chen H, Lan Z, Li Q and Li Y: Abnormal expression of long noncoding RNA FGD5-AS1 affects the development of periodontitis through regulating miR-142-3p/SOCS6/NF-κB pathway. Artif Cells Nanomed Biotechnol 47: 2098-2106, 2019.
11. Xi X, Chu Y, Liu N, Wang Q, Yin Z, Lu Y and Chen Y: Joint bioinformatics analysis of underlying potential functions of hsa-let-7b-5p and core genes in human glioma. J Transl Med 17: 129, 2019.
12. Chen JQ, Papp G, Szodoray P and Zeher M: The role of microRNAs in the pathogenesis of autoimmune diseases. Autoimmun Rev 15: 1171-1180, 2016.
13. Zeng L, Cui J, Wu H and Lu Q: The emerging role of circulating microRNAs as biomarkers in autoimmune diseases. Autoimmunity 47: 419-429, 2014.
14. Feng Y, Niu LL, Wei W, Zhang WY, Li XY, Cao JH and Zhao SH: A feedback circuit between miR-133 and the ERK1/2 pathway involving an exquisite mechanism for regulating myoblast proliferation and differentiation. Cell Death Dis 4: e934, 2013.
15. Navickas R, Gal D, Laucevičius A, Taparauskaitė A, Zdanytė M and Holvoet P: Identifying circulating microRNAs as biomarkers of cardiovascular disease: A systematic review. Cardiovasc Res 111: 322-337, 2016.
16. Dong Y, Zhao J, Wu CW, Zhang L, Liu X, Kang W, Leung WW, Zhang N, Chan FK, Sung JJ, *et al*: Tumor suppressor functions of miR-133a in colorectal cancer. Mol Cancer Res 11: 1051-1060, 2013.
17. Cui W, Zhang S, Shan C, Zhou L and Zhou Z: MicroRNA-133a regulates the cell cycle and proliferation of breast cancer cells by targeting epidermal growth factor receptor through the EGFR/Akt signaling pathway. FEBS J 280: 3962-3974, 2013.
18. Yamasaki T, Yoshino H, Enokida H, Hidaka H, Chiyomaru T, Nohata N, Kinoshita T, Fuse M, Seki N and Nakagawa M: Novel molecular targets regulated by tumor suppressors microRNA-1 and microRNA-133a in bladder cancer. Int J Oncol 40: 1821-1830, 2012.
19. Tsunoda SP, Wiesner B, Lorenz D, Rosenthal W and Pohl P: Aquaporin-1, nothing but a water channel. J Biol Chem 279: 11364-11367, 2004.
20. Shanahan CM, Connolly DL, Tyson KL, Cary NR, Osbourn JK, Agre P and Weissberg PL: Aquaporin-1 is expressed by vascular smooth muscle cells and mediates rapid water transport across vascular cell membranes. J Vasc Res 36: 353-362, 1999.
21. Verkman AS: More than just water channels: Unexpected cellular roles of aquaporins. J Cell Sci 118: 3225-3232, 2005.

22. Liu K, Tsujimoto H, Cha SJ, Agre P and Rasgon JL: Aquaporin water channel AgAQP1 in the malaria vector mosquito anopheles gambiae during blood feeding and humidity adaptation. Proc Natl Acad Sci USA 108: 6062-6066, 2011.
23. Yamazato Y, Shiozaki A, Ichikawa D, Kosuga T, Shoda K, Arita T, Konishi H, Komatsu S, Kubota T, Fujiwara H, *et al*: Aquaporin 1 suppresses apoptosis and affects prognosis in esophageal squamous cell carcinoma. Oncotarget 9: 29957-29974, 2018.
24. Tomita Y, Dorward H, Yool AJ, Smith E, Townsend AR, Price TJ and Hardingham JE: Role of aquaporin 1 signalling in cancer development and progression. Int J Mol Sci 18: 299, 2017.
25. Qin F, Zhang H, Shao Y, Liu X, Yang L, Huang Y, Fu L, Gu F and Ma Y: Expression of aquaporin1, a water channel protein, in cytoplasm is negatively correlated with prognosis of breast cancer patients. Oncotarget 7: 8143-8154, 2016.
26. Livak KJ and Schmittgen TD: Analysis of relative gene expression data using real-time quantitative PCR and the 2(-Delta Delta C(T)) method. Methods 25: 402-408, 2001.
27. Ogino H, Fujii M, Ono M, Maezawa K, Kizu J and Hori S: In vivo and in vitro effects of fluoroquinolones on lipopolysaccharide-induced pro-inflammatory cytokine production. J Infect Chemother 15: 168-173, 2009.
28. Skelly DT, Hennessy E, Dansereau MA and Cunningham C: A systematic analysis of the peripheral and CNS effects of systemic LPS, IL-1β, [corrected] TNF-α and IL-6 challenges in C57BL/6 mice. PLoS One 8: e69123, 2013. Erratum in: PLoS One 8: 10.1371/annotation/90c76048-2edd-4315-8404-4d9d8cbd411e, 2013.
29. Eggesbø JB, Hjermann I, Høstmark AT and Kierulf P: LPS induced release of IL-1 beta, IL-6, IL-8 and TNF-alpha in EDTA or heparin anticoagulated whole blood from persons with high or low levels of serum HDL. Cytokine 8: 152-160, 1996.
30. Hotchkiss RS, Moldawer LL, Opal SM, Reinhart K, Turnbull IR and Vincent JL: Sepsis and septic shock. Nat Rev Dis Primers 2: 16045, 2016.
31. Iba T, Watanabe E, Umemura Y, Wada T, Hayashida K, Kushimoto S; Japanese Surviving Sepsis Campaign Guideline Working Group for disseminated intravascular coagulation and Wada H: Sepsis-associated disseminated intravascular coagulation and its differential diagnoses. J Intensive Care 7: 32, 2019.
32. Prescott HC and Angus DC: Enhancing recovery from sepsis: A review. JAMA 319: 62-75, 2018.
33. Reinhart K, Daniels R, Kissoon N, Machado FR, Schachter RD and Finfer S: Recognizing sepsis as a global health priority-a WHO resolution. N Engl J Med 377: 414-417, 2017.
34. Giza DE, Fuentes-Mattei E, Bullock MD, Tudor S, Goblirsch MJ, Fabbri M, Lupu F, Yeung SJ, Vasilescu C and Calin GA: Cellular and viral microRNAs in sepsis: Mechanisms of action and clinical applications. Cell Death Differ 23: 1906-1918, 2016.
35. Hombach S and Kretz M: Non-coding RNAs: Classification, biology and functioning. In: Non-coding RNAs in colorectal cancer, Springer, pp3-17, 2016.
36. Zhang CC and Niu F: LncRNA NEAT1 promotes inflammatory response in sepsis-induced liver injury via the Let-7a/TLR4 axis. Int Immunopharmacol 75: 105731, 2019.
37. Chen Y, Fu Y, Song YF and Li N: Increased expression of lncRNA UCA1 and HULC is required for pro-inflammatory response during LPS induced sepsis in endothelial cells. Front Physiol 10: 608, 2019.
38. Fang Y, Hu JF, Wang ZH, Zhang SG, Zhang RF, Sun LM, Cui HW and Yang F: GAS5 promotes podocyte injury in sepsis by inhibiting PTEN expression. Eur Rev Med Pharmacol Sci 22: 8423-8430, 2018.
39. Lan C, Shi X, Guo N, Pei H and Zhang H: Value of serum miR-155-5p and miR-133a-3p expression for the diagnosis and prognosis evaluation of sepsis. Zhonghua Wei Zhong Bing Ji Jiu Yi Xue 28: 694-698, 2016 (In Chinese).
40. Ahn J and Kim J: Mechanisms and consequences of inflammatory signaling in the myocardium. Curr Hypertens Rep 14: 510-516, 2012.
41. Fang L, Moore XL, Dart AM and Wang LM: Systemic inflammatory response following acute myocardial infarction. J Geriatr Cardiol 12: 305-312, 2015.
42. Hochstadt A, Meroz Y and Landesberg G: Myocardial dysfunction in severe sepsis and septic shock: More questions than answers? J Cardiothorac Vasc Anesth 25: 526-535, 2011.
43. Pathan N, Franklin JL, Eleftherohorinou H, Wright VJ, Hemingway CA, Waddell SJ, Griffiths M, Dennis JL, Relman DA, Harding SE and Levin M: Myocardial depressant effects of interleukin 6 in meningococcal sepsis are regulated by p38 mitogen-activated protein kinase. Crit Care Med 39: 1692-1711, 2011.
44. Marchini G, Ståbi B, Kankes K, Lonne-Rahm S, Østergaard M and Nielsen S: AQP1 and AQP3, psoriasin, and nitric oxide synthases 1-3 are inflammatory mediators in erythema toxicum neonatorum. Pediatr Dermatol 20: 377-384, 2003.
45. Trujillo E, González T, Marin R, Martin-Vasallo P, Marples D and Mobasheri A: Human articular chondrocytes, synoviocytes and synovial microvessels express aquaporin water channels; upregulation of AQP1 in rheumatoid arthritis. Histol Histopathol 19: 435-444, 2004.
46. Rana S, Shahzad M and Shabbir A: Pistacia integerrima ameliorates airway inflammation by attenuation of TNF-α, IL-4, and IL-5 expression levels, and pulmonary edema by elevation of AQP1 and AQP5 expression levels in mouse model of ovalbumin-induced allergic asthma. Phytomedicine 23: 838-845, 2016.